



Calhoun: The NPS Institutional Archive
DSpace Repository

Faculty and Researchers

Faculty and Researchers' Publications

2017

Minimum Power Slews and the James Webb Space Telescope

Karpenko, Mark; Dennehy, Cornelius J.; Marsh, Harleigh C.; Gong, Qi

AAS/A/AA

Karpenko, M., Dennehy, C.J., Marsh, H.C. and Qi Gong. "Minimum Power Slews and the James Webb Space Telescope", 27th AAS/A/AA Space Flight Mechanics Meeting, Volume 160, Advances in the Astronautical Sciences, 2017.

<http://hdl.handle.net/10945/66174>

This publication is a work of the U.S. Government as defined in Title 17, United States Code, Section 101. As such, it is in the public domain, and under the provisions of Title 17, United States Code, Section 105, it may not be copyrighted.

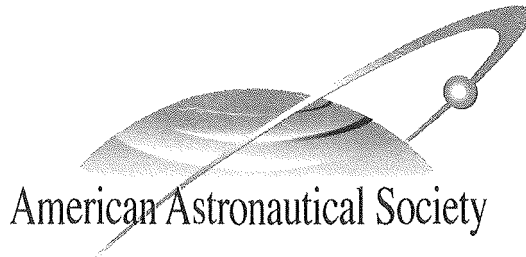
Downloaded from NPS Archive: Calhoun



Calhoun is the Naval Postgraduate School's public access digital repository for research materials and institutional publications created by the NPS community. Calhoun is named for Professor of Mathematics Guy K. Calhoun, NPS's first appointed -- and published -- scholarly author.

Dudley Knox Library / Naval Postgraduate School
411 Dyer Road / 1 University Circle
Monterey, California USA 93943

<http://www.nps.edu/library>



SPACEFLIGHT MECHANICS 2017

Volume 160

Part III

ADVANCES IN THE ASTRONAUTICAL SCIENCES

Edited by
Jay W. McMahon
Yanping Guo
Frederick A. Leve
Jon A. Sims

*Proceedings of the 27th AAS/AIAA Space
Flight Mechanics Meeting held February 5–9,
2017, San Antonio, Texas, U.S.A.*

*Published for the American Astronautical Society by
Univelt, Incorporated, P.O. Box 28130, San Diego, California 92198
Web Site: <http://www.univelt.com>*

Copyright 2017

by

AMERICAN ASTRONAUTICAL SOCIETY

AAS Publications Office
P.O. Box 28130
San Diego, California 92198

Affiliated with the American Association for the Advancement of Science
Member of the International Astronautical Federation

First Printing 2017

Library of Congress Card No. 57-43769

ISSN 1081-6003

ISBN 978-0-87703-637-1 (Hard Cover Plus CD ROM)
ISBN 978-0-87703-638-8 (Digital Version)

Published for the American Astronautical Society
by Univelt, Incorporated, P.O. Box 28130, San Diego, California 92198
Web Site: <http://www.univelt.com>

Printed and Bound in the U.S.A.

MINIMUM POWER SLEWS AND THE JAMES WEBB SPACE TELESCOPE

Mark Karpenko,^{*} Cornelius J. Dennehy,[†] Harleigh C. Marsh[‡] and Qi Gong[§]

Power is a precious commodity in space flight. Reducing the power demands of reaction wheels during spacecraft attitude slews can have multiple benefits both in the up-front spacecraft design phase as well as during in-flight operations. In an effort to reduce power requirements of momentum control systems, many authors have contemplated the use of proxies for reaction wheel power to design *minimal effort* slews. Proxies for power are used because the power input equation is non-smooth leading to a seemingly unsolvable problem in optimal control. In this paper we show, through the application of various transformations and the introduction of appropriate functional constraints, that a smooth cost functional for reaction wheel input power can indeed be built. Standard techniques can then be used to solve and analyze the power optimal slew problem. The concept is applied to reduce the power requirements for a typical large-angle slew of the James Webb Space Telescope. The energy reduction ($\sim 20\%$) is obtained by finding a minimum power momentum distribution that achieves the necessary control effort while simultaneously reducing power input to the individual wheels.

INTRODUCTION

Reducing reaction wheel power requirements is a desirable objective in the implementation of spacecraft attitude control systems. Accordingly, many authors have investigated techniques for designing *effort* optimal attitude maneuvers. We emphasize the term *effort* to draw attention to the fact that in the literature, the true reaction wheel power consumption is not minimized – only cost functionals that represent proxies for power. For example, a feedback solution was developed in [1] to minimize the L^2 norm of the instantaneous mechanical energy (torque times angular rate) of a redundant reaction wheel array. While the mechanical energy can represent a significant component of the total power consumption, it is not the only term in the power equation. Regenerative energy

^{*} Research Associate Professor and corresponding author, Department of Mechanical and Aerospace Engineering, Naval Postgraduate School, Monterey, California 93943, U.S.A. E-mail: mkarpenk@nps.edu.

[†] NASA Technical Fellow, Guidance, Navigation and Control, NASA Engineering and Safety Center, NASA Goddard Space Flight Center (GSFC), Greenbelt, Maryland 20771, U.S.A.

[‡] Graduate Student., Department of Applied Mathematics and Statistics, University of California Santa Cruz, Santa Cruz, California 95064, U.S.A.

[§] Associate Professor, Department of Applied Mathematics and Statistics, University of California Santa Cruz, Santa Cruz, California 95064, U.S.A.

optimal reaction wheel attitude control was investigated in [2], again using mechanical energy as a cost functional. In practice, however, regeneration is not employed on current spacecraft systems and it is not clear if such solutions remain valid when generated current is shunted to ground. Similarly in [3,4], the proxy for reaction wheel power was assumed to be the square of the wheel mechanical power and in [5] the current-squared times resistance (copper-loss) was used instead. Instantaneous friction losses were considered in addition to mechanical power in [6] as part of a dissipative power reduction control allocation scheme for momentum control systems. A version of the power cost functional was also considered in [7] where it was shown that under certain operational conditions, e.g. a redundant reaction wheel array with fixed wheel speed bias, the reaction wheel power input equation can be reduced to a certain quadratic form.

There are both up-front design benefits and in-flight operational advantages (especially late in the mission life) to be gained by applying methods to minimize reaction wheel power consumption, rather than proxies for power, during spacecraft attitude slews. One of the up-front design benefits of minimizing the wheel power demands on any given spacecraft is centered on simplifying the design of the electrical channels servicing the reaction wheels. Consider, for example, the fact that executing a maneuver (particularly a large-angle slew) may cause large but short-term power demands. This can generate electrical transients/surges that can degrade power quality across the entire main electrical bus of the vehicle. On some spacecraft, the main bus may not only service the reaction wheels, but also the delicate on-board science instruments so great care must be taken in the design of the spacecraft electrical system.

Typically, the electrical channels feeding power to the reaction wheels are sized for the predicted wheel peak power requirements. On some spacecraft, this may necessitate electrical service to the reaction wheels as high as 10 Amps. Designing sufficient over-current protections in such power systems, where the wheel peak-to-average power draw ratio is much greater than one, is often problematic and nuisance over-current trips can become troublesome during in-flight operations. Minimizing reaction wheel power demands and energy consumption could allow for operations in which the reaction wheel peak-to-average power draw ratio is closer to unity. This would simplify the design of the reaction wheel electrical feed channels. Reducing the reaction wheel power demands could also influence battery sizing since these energy storage devices are typically sized to accommodate the requirements of high spacecraft slew rates. Thus, mass savings could be realized in the power distribution components and the electrical bus cabling as well as in the batteries.

From an operational point of view, reducing reaction wheel energy consumption during the large-angle attitude slews could have the benefit of lowering the induced thermal stresses within the wheels themselves: both in the wheel drive electronics and in the wheel bearing/lubrication system. This may have the positive impact of prolonging the life expectancy of the wheels. Such a consideration is important for a spacecraft like the James Webb Space Telescope (JWST) which will be expected to perform its science mission for more than a decade, particularly in light of the recent failures of the reaction wheels on NASA's Dawn, Mars Odyssey, and Kepler spacecraft.⁸

The ability to perform large attitude slews for science encounters late in mission life, can also be enhanced by reducing reaction wheel power requirements. Consider that late in a spacecraft's mission life, the power system margins can become degraded so that a peak power load (e.g., during a large-angle slew) may create electrical transients that are larger than the power system can accommodate while still maintaining an acceptable power quality. By minimizing reaction wheel energy demands, science operations could continue well after the end of the primary mission duration because large attitude slews could still be performed despite diminished or degraded power generation/energy storage capabilities.

The most compelling benefits to be gained from reducing reaction wheel power demands come from: (i) simplifying the electrical power system branch circuits servicing the reaction wheels, (ii) improvements in the spacecraft's power quality system-wide, (iii) reduced electrical transients/surges as seen by the battery energy storage elements or the science instruments, and (iv) the potential for prolonging the useful mission life of a spacecraft. Thus, minimizing reaction wheel power is an important problem. Yet in the literature, only proxies for power have been considered. This is primarily because the former problem is a difficult to solve non-smooth optimal control problem. A non-smooth optimal control problem has terms that are non-differentiable with respect to their arguments. Solution of such problems by the application of Pontryagin's Minimum Principle requires the use of complicated non-smooth analysis,^{9,10} which motivates the desire to work instead with various quadratic proxies for power. In this paper, we show how a smooth cost functional based on the reaction wheel power input equation can be built through the application of various transformations. By generating a smooth optimal control problem from the original non-smooth problem, standard techniques, e.g. Pseudospectral optimal control theory [11], can be applied to obtain a solution so that the various terms comprising the power input equation can be properly accounted for.

As an application example, we consider attitude slewing of the JWST and present the development of minimum power slews for reaction wheel spacecraft. The JWST was chosen as an example because the spacecraft is expected to have a long mission life. Exploring power reduction strategies is thus a relevant and practical engineering problem since the results could be used to prolong life expectancy or enhance end of mission operations. Moreover, the JWST employs a redundant array of six reaction wheels for attitude control. This redundancy creates a tradespace that can be exploited for reaction wheel power reduction even when maneuvers are constrained to the Eigenaxis. It is shown that current attitude control systems are not power optimal and that significant reductions in power requirements (approximately 20% for the example problem presented here). The power reduction is obtained by appropriate adjustments to the slew momentum profile and proper re-allocation of the individual reaction wheel controls.

In the remainder of the paper, we describe the attitude dynamics of the JWST and develop an appropriate model for reaction wheel power. We then show how minimizing reaction wheel power can be cast as a non-smooth L^1 optimal control problem and describe the details for transforming this problem into a smooth problem formulation. The results are then applied to determine a canonical minimum power large-angle slew for the JWST that is compared against the conventional strategy for slewing the spacecraft.

ATTITUDE DYNAMICS OF THE JWST

The JWST is the scientific successor to the Hubble Space Telescope. An artist's rendition of the spacecraft is shown in Figure 1. While the Hubble Space Telescope collects primarily optical and ultraviolet wavelengths, the JWST will collect infrared wavelengths and with greater sensitivity in order to extend the discoveries of the Hubble Space Telescope and carry out its four key scientific mission goals.¹² The mission duration is designed to be at least 5 years, but could be longer than 10 years depending on fuel reserves and the rate at which the spacecraft's components degrade in the space environment. The JWST will orbit the Sun at the second Lagrange point (L2) of the Earth-Sun system.

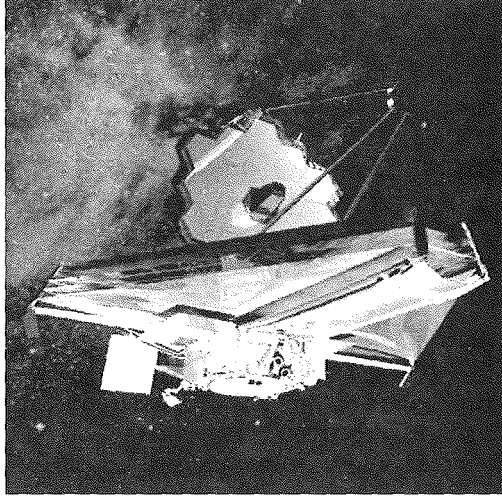


Figure 1. Artist's rendering of the James Webb Space Telescope (JWST).

Attitude control of the JWST is done using reaction wheels for slew and thrusters for momentum management/orbit maintenance. The rotational dynamics of the space telescope can be derived by considering the conservation of angular momentum in the inertial frame:

$$\mathbf{H}^N(t) = \int_0^t \boldsymbol{\tau}_{\text{ext}}^N(t) dt + \mathbf{H}_0^N \quad (1)$$

where $\mathbf{H}^N(t)$ is the total angular momentum of the spacecraft at time t expressed in the inertial frame, N , and $\boldsymbol{\tau}_{\text{ext}}^N(t)$ is the vector of time-varying externally applied torques (e.g. solar radiation pressure), also expressed in the N frame.

Differentiating (1), the following equation is obtained

$$\dot{\mathbf{H}}^N = \dot{\mathbf{H}}^B + \boldsymbol{\omega} \times \mathbf{H}^B = \boldsymbol{\tau}_{\text{ext}}^N \quad (2)$$

where $\boldsymbol{\omega}$ is the angular rate of the spacecraft expressed in the body frame. The angular momentum of the spacecraft and its reaction wheel system is given, in the body frame, as

$$\mathbf{H}^B = \mathbf{J}\boldsymbol{\omega} + \mathbf{Z}\mathbf{h} \quad (3)$$

In (3), matrix \mathbf{J} is the inertia tensor of the spacecraft with freely rotating reaction wheels and matrix-vector product $\mathbf{Z}\mathbf{h}$ is the total angular momentum associated with an array of n reaction wheels. The $3 \times n$ reaction wheel transformation matrix $\mathbf{Z} = [\mathbf{z}_1 | \mathbf{z}_2 | \dots | \mathbf{z}_n]$ gives the orientation of the spin axis of each reaction wheel with respect to the spacecraft coordinate system. The product $\mathbf{Z}\mathbf{h}$, where $\mathbf{h} = [h_1, h_2, \dots, h_n]^T$, therefore represents the transformation of the reaction wheel momentum from the individual actuator frames to the body-fixed frame. The JWST uses an array of six reaction wheels so the attitude control system is over actuated. For such a control system, there is a theoretically infinite number of ways in which the commanded body-axis control torques can be allocated to the wheels, although least-squares allocation is normally used. Redundancy in actuation provides a natural mechanism for reducing the energy consumption of the array.

As it is convenient to work in the body-fixed frame, equation (2) is expanded (using eq. 3) and rearranged to give

$$\mathbf{J}\dot{\boldsymbol{\omega}} + \mathbf{Z}\dot{\mathbf{h}} + \boldsymbol{\omega} \times (\mathbf{J}\boldsymbol{\omega} + \mathbf{Z}\mathbf{h}) = \boldsymbol{\tau}_{\text{env}} + \boldsymbol{\tau}_{\text{RCS}} \quad (4)$$

where the external torque $\boldsymbol{\tau}_{\text{ext}}^N = \boldsymbol{\tau}_{\text{env}} + \boldsymbol{\tau}_{\text{RCS}}$ has been expanded into an expression involving the environmental torque plus the torque due to the spacecraft reaction control system (RCS). These two torques are naturally expressed as vectors in the body-fixed coordinate frame. However, since the RCS is only used for momentum dumping and the environmental torques are small, it is reasonable to assume that the sum $\boldsymbol{\tau}_{\text{env}} + \boldsymbol{\tau}_{\text{RCS}}$ is null during the course of a slewing maneuver.

We now turn our attention to the dynamics of the reaction wheel. The angular momentum of each reaction wheel about its axis of rotation is

$$h_i = J_i \Omega_i - J_i \mathbf{z}_i^T \boldsymbol{\omega} \quad (5)$$

where J_i is the inertia of reaction wheel i about its spin axis, and Ω_i is the angular rate of the reaction wheel relative to the actuator frame. The product $J_i \mathbf{z}_i^T \boldsymbol{\omega}$ accounts for the change in angular momentum arising due to the relative motion between the spinning rotors and the spacecraft body. Noting that the reaction wheel control torque is $\tau_w = J\dot{\Omega}$, the differential equation describing the reaction wheel dynamics can be written as¹³

$$\dot{h}_i = \tau_{w,i} - J_i \mathbf{z}_i^T \dot{\boldsymbol{\omega}} \quad (6)$$

Combining (4) and (6), the rotational dynamics can be written in the following matrix form

$$\begin{bmatrix} \dot{\boldsymbol{\omega}} \\ \dot{\mathbf{h}} \end{bmatrix} = \boldsymbol{\Gamma}^{-1} \begin{bmatrix} -\boldsymbol{\omega} \times (\mathbf{J}\boldsymbol{\omega} + \mathbf{Z}\mathbf{h}) \\ \mathbf{u} \end{bmatrix} \quad (7)$$

where

$$\boldsymbol{\Gamma} = \begin{bmatrix} \mathbf{J} & \mathbf{Z} \\ \mathbf{J}_w \mathbf{Z}^T & \mathbf{I}_{6 \times 6} \end{bmatrix} \quad (8)$$

where $\mathbf{J}_w = \text{diag}([J_1, J_2, \dots, J_6])$ is a diagonal matrix of reaction wheel rotor inertias and $\mathbf{I}_{6 \times 6}$ is a 6×6 identity matrix. The control vector is taken as $\mathbf{u} = [\tau_{w,1}, \tau_{w,2}, \dots, \tau_{w,6}]^T$.

To complete the mathematical model of the spacecraft dynamics, the differential equations for the attitude kinematics are defined in terms of quaternions. The relevant differential equations are¹⁴

$$\dot{\mathbf{q}} = \frac{1}{2} \mathbf{Q}(\boldsymbol{\omega}) \mathbf{q} \quad (9)$$

where the skew-symmetric matrix $\mathbf{Q}(\boldsymbol{\omega})$ is given as

$$\mathbf{Q}(\boldsymbol{\omega}) = \begin{bmatrix} 0 & \omega_3 & -\omega_2 & \omega_1 \\ -\omega_3 & 0 & \omega_1 & \omega_2 \\ \omega_2 & -\omega_1 & 0 & \omega_3 \\ -\omega_1 & -\omega_2 & -\omega_3 & 0 \end{bmatrix} \quad (10)$$

REACTION WHEEL POWER

The power consumption of a reaction wheel may be derived by considering the electrical equations of a direct-current (DC) motor operating in the steady state.¹⁵ In such a model, the load-torque

is the sum of the torque commanded by the attitude control system, τ_{cmd} , and a friction term associated with the reaction wheel drag, τ_{drag} . In the steady-state, the load-torque must be balanced against the average current, I , flowing through the motor windings:

$$I = \frac{1}{K_T} (\tau_{\text{cmd}} + \tau_{\text{drag}}) \quad (11)$$

where K_T is the so-called motor torque constant. The drag torque comprises both a Coulomb and viscous term $\tau_{\text{drag}} = \beta_1 \text{sign}(\Omega) + \beta_2 \Omega$ where β_1 and β_2 are constants for a given wheel and Ω is the reaction wheel angular rate. The term involving the sign of the wheel rate accounts for the directional effect of the Coulomb friction component.

The equation describing the supply voltage drop across the reaction wheel electrical harness and drive motor is

$$V_s = IR + K_\Omega \Omega \quad (12)$$

where V_s is the supply voltage, R is the combined harness and winding resistance, K_Ω is the back electromotive force (EMF) constant. The power input, $\mathcal{P} = IV_s$ to the reaction wheel is, therefore

$$\mathcal{P} = \frac{R}{K_T^2} (\tau_{\text{cmd}} + \beta_1 \text{sign}(\Omega) + \beta_2 \Omega)^2 + \frac{K_\Omega}{K_T} \Omega (\tau_{\text{cmd}} + \beta_1 \text{sign}(\Omega) + \beta_2 \Omega) + P_q \quad (13)$$

where additional term, P_q , represents the quiescent draw associated with the electronics. We note that when the reaction wheel behaves as a generator, such as when a wheel is decelerated, $\mathcal{P} \leq 0$ in (13). In a typical attitude control system, generated power is not recovered and is instead shunted to ground via a ballast resistor. Hence, bus power is only utilized by the reaction wheel when $\mathcal{P} > 0$. Thus, the total electric power input to an array of n reaction wheels, at a given instant in time, is simply the sum over the wheels

$$\mathcal{P}_{\text{array}} = \sum_{i=1}^n \{\mathcal{P}_i\}^+, \quad (14)$$

where operator $\{\mathcal{P}_i\}^+$ is defined as

$$\{\mathcal{P}_i\}^+ = \begin{cases} \mathcal{P}_i, & \text{if } \mathcal{P}_i > 0 \\ 0, & \text{if } \mathcal{P}_i \leq 0 \end{cases} \quad (15)$$

From (13) and (15) it is apparent that reaction wheel power input is a non-smooth function. Thus, a cost functional for minimizing energy over a slew, for example minimizing the cumulative power $J = \int_0^{t_{\text{slew}}} \mathcal{P}_{\text{array}}(t) dt$, is non-differentiable with respect to its arguments. This creates challenges not only in solving the associated optimal control problem, but also in analyzing the necessary conditions for optimality which is required to validate the solution. However as will be seen later, minimizing reaction wheel power can be interpreted as an L^1 -optimal control problem. Although the cost functional of an L^1 -optimal control problem is also non-smooth, we show in the next section how the solution to an L^1 problem can be determined using smooth analysis and existing computational tools.

L^1 OPTIMAL CONTROL CONCEPTS

The cost functional of an L^1 -optimal control problem is nonsmooth as it is non-differentiable with respect to its arguments. Rather than invoking the machinery of nonsmooth calculus (see

Clarke^{9,10}), an alternative is to transform the problem into a smooth one and then apply Pontryagin's principle as outlined in reference [16]. To familiarize the reader with the approach, a simplified version of the minimum power attitude control problem will be developed and analyzed in this section. The same concepts will then be utilized in the sequel, to minimize energy consumption of the 6-reaction wheel array of the JWST.

Consider a standard 4-wheel pyramid²⁰ which has a 3×4 transformation matrix given by

$$\mathbf{Z} = \begin{bmatrix} \sin(\eta) & \sin(\eta) & \sin(\eta) & \sin(\eta) \\ 0 & \cos(\eta) & 0 & -\cos(\eta) \\ \cos(\eta) & 0 & -\cos(\eta) & 0 \end{bmatrix} \quad (16)$$

where angle η is the elevation angle of the wheel spin axes from the yz -plane. As is apparent from (16), the wheels are uniformly distributed about the x -axis.

In order to slew a spacecraft, the wheels are used to exchange momentum with the vehicle as described earlier. Recall that the angular momentum of the spacecraft is given, in the body frame, as

$$\mathbf{H}^B = \mathbf{J}\boldsymbol{\omega} + \mathbf{Z}\mathbf{h} \quad (17)$$

If it is assumed, for simplicity, that the attitude control system has a zero momentum bias, i.e. $\mathbf{H}^B = \mathbf{0}$, then (17) may be rearranged to give

$$\boldsymbol{\omega} = -\mathbf{J}^{-1}\mathbf{Z}\mathbf{h} \quad (18)$$

Now, consider an attitude maneuver about the spacecraft body x -axis. In this case, (18) can be expanded as follows

$$\begin{bmatrix} \omega_x \\ 0 \\ 0 \end{bmatrix} = \begin{bmatrix} -\frac{1}{J_{xx}} \sin(\eta) (h_1 + h_2 + h_3 + h_4) \\ \cos(\eta) (h_2 - h_4) \\ \cos(\eta) (h_1 - h_3) \end{bmatrix} \quad (19)$$

A diagonal inertia tensor has been assumed.

From (19), it is evident that $h_1 = h_3$ and $h_2 = h_4$ due to the geometry of the reaction wheel array. Thus, a simplified dynamical model for the attitude maneuver can be written as

$$\begin{bmatrix} \dot{\theta} \\ \dot{\bar{h}} \end{bmatrix} = \begin{bmatrix} K\bar{h} \\ \bar{\tau} \end{bmatrix} \quad (20)$$

where $K = -\frac{2}{J_{xx}} \sin(\eta)$, $\bar{h} = h_1 + h_2$, and $\bar{\tau} = \tau_1 + \tau_2$. Noting that $\bar{h} = J_w \bar{\Omega}$, and that optimization is invariant under scalar multiplication by J_w , the following *minimum effort* rest-to-rest slew problem can be formulated

$$P_{NS} : \left\{ \begin{array}{ll} \text{Minimize} & J[\mathbf{x}(\cdot), \mathbf{u}(\cdot), t_f] = \int_0^{t_f} |\bar{\tau}(t)\bar{h}(t)| dt \\ \text{Subject to} & \dot{\mathbf{x}} = \begin{bmatrix} K\bar{h} \\ \bar{\tau} \end{bmatrix} \\ & \mathbf{u} = \bar{\tau} \\ & \mathbf{x}(t_0) = [0, 0]^T \\ & \mathbf{x}(t_f) = [\theta_{\text{slew}}, 0]^T \\ & \bar{\tau}^L \leq \bar{\tau} \leq \bar{\tau}^U \\ & t_f = t_{\text{slew}} \end{array} \right. \quad (21)$$

where θ_{slew} and t_{slew} are the slew angle and slew time, respectively. Nonsmooth problem P_{NS} is a particular case of a general minimum energy problem¹⁶ and it's solution is analogous to minimizing the L^1 measure of the reaction wheel mechanical power.

In order to apply Pontryagin's principle to solve problem P_{NS} , non-smooth analysis can be used.^{9,10} Alternatively, the problem may be transformed into an equivalent smooth problem by introducing additional variables and constraints as part of the problem formulation. To proceed, we first split the cost functional into its positive and negative parts. Following [16], let

$$z(t) := \bar{\tau}(t)\bar{h}(t) \quad (22)$$

We may now write

$$z(t) = z_a(t) - z_b(t) \quad (23)$$

where $z_a(t) = \{z(t)\}^+$ and $z_b(t) = \{-z(t)\}^+$ represent the positive and negative parts of $z(t)$.

The notation used implies that $z_a(t) \geq 0$ and $z_b(t) \geq 0$, from which it follows that

$$|z(t)| = z_a(t) + z_b(t) \quad (24)$$

Using the above, the original nonsmooth minimum effort problem (21) can be re-cast as a smooth problem by introducing the variables z_a and z_b and incorporating the appropriate constraints

$$P_S : \left\{ \begin{array}{ll} \text{Minimize} & J[\mathbf{x}(\cdot), \mathbf{u}(\cdot), t_f] = \int_0^{t_f} (z_a(t) + z_b(t)) dt \\ \text{Subject to} & \dot{\mathbf{x}} = \begin{bmatrix} K\bar{h} \\ \bar{\tau} \end{bmatrix} \\ & \mathbf{u} = [\bar{\tau}, z_a, z_b]^T \\ & \mathbf{x}(t_0) = [0, 0]^T \\ & \mathbf{x}(t_f) = [\theta_{\text{slew}}, 0]^T \\ & z_a(t) \geq 0 \\ & z_b(t) \geq 0 \\ & 0 \leq z_a(t) - \bar{h}(t)\bar{\tau}(t) \\ & 0 \leq z_b(t) + \bar{h}(t)\bar{\tau}(t) \\ & t_f = t_{\text{slew}} \end{array} \right. \quad (25)$$

Pontryagin's principle is now applied to the smooth problem P_S in order to develop the necessary conditions for optimality. According to Pontryagin's principle, the Hamiltonian must be minimized at each instant of time. Because problem P_S involves box and other constraints on the control, the standard Karush-Kuhn-Tucker (KKT) conditions must be applied by developing the Lagrangian of the Hamiltonian¹⁶

$$\bar{H}(\boldsymbol{\mu}, \boldsymbol{\lambda}, \mathbf{x}, \mathbf{u}) = H(\boldsymbol{\lambda}, \mathbf{x}, \mathbf{u}) + \boldsymbol{\mu}^T \mathbf{h}(\mathbf{x}, \mathbf{u}) \quad (26)$$

where $H(\boldsymbol{\lambda}, \mathbf{x}, \mathbf{u})$ is the control Hamiltonian, $\boldsymbol{\mu}$ is the path covector, and \mathbf{h} is the vector of path constraints. The Lagrangian of the Hamiltonian is minimized if it is stationary with respect to the control vector, \mathbf{u} and the multiplier-constraint pair satisfies the complementarity condition. That is, the following must be satisfied at each instant of time:

$$\frac{\partial \bar{H}}{\partial \mathbf{u}} = \frac{\partial H}{\partial \mathbf{u}} + \boldsymbol{\mu}^T \left(\frac{\partial \mathbf{h}}{\partial \mathbf{u}} \right) = 0 \quad (27)$$

and

$$\mu_i \begin{cases} \leq 0 & \text{if } h_i = h_i^L \\ = 0 & \text{if } h_i^L \leq h_i \leq h_i^U \\ \geq 0 & \text{if } h_i = h_i^U \end{cases} \quad (28)$$

For the minimum effort problem, P_S , the Lagrangian of the Hamiltonian is

$$\bar{H}(\boldsymbol{\mu}, \boldsymbol{\lambda}, \mathbf{x}, \mathbf{u}) = z_a + z_b + \lambda_\theta K \bar{h} + \lambda_h \bar{h} + \mu_\tau \bar{\tau} + \mu_a z_a + \mu_b z_b + \mu_{\text{pos}} (z_a - \bar{h} \bar{\tau}) + \mu_{\text{neg}} (z_b + \bar{h} \bar{\tau}) \quad (29)$$

Application of (27) yields the following stationarity conditions,

$$\frac{\partial \bar{H}}{\partial \bar{\tau}} = \lambda_h + \mu_\tau - \mu_{\text{pos}} \bar{h} + \mu_{\text{neg}} \bar{h} = 0 \quad (30)$$

$$\frac{\partial \bar{H}}{\partial z_a} = 1 + \mu_a + \mu_{\text{pos}} = 0 \quad (31)$$

$$\frac{\partial \bar{H}}{\partial z_b} = 1 + \mu_b + \mu_{\text{neg}} = 0 \quad (32)$$

The adjoint equations, $-\dot{\boldsymbol{\lambda}} = \frac{\partial \bar{\mathcal{H}}}{\partial \mathbf{x}}$, provide the following relationships between the state-costate pairs of the minimized Hamiltonian

$$\dot{\lambda}_\theta = 0 \quad (33)$$

$$\dot{\lambda}_h = -\lambda_\theta K + \mu_{\text{pos}} \bar{\tau} - \mu_{\text{neg}} \bar{\tau} \quad (34)$$

From (33), it is apparent that the value of λ_θ is a constant when the Hamiltonian is minimized.

The terminal transversality conditions, $\boldsymbol{\lambda}(t_f) = \frac{\partial \bar{E}}{\partial \mathbf{x}(t_f)}$, are evaluated by constructing the endpoint Lagrangian

$$\bar{E} = \nu_t(t_f - t_{\text{slew}}) + \nu_\theta(\theta_f - \theta_{\text{slew}}) + \nu_h(\bar{h}_f - 0) \quad (35)$$

where $\boldsymbol{\nu}$ is a vector of multipliers on the endpoint functions. Since the values of $\boldsymbol{\nu}$ are not known *a priori*, the partial derivatives of (35) are not particularly useful. However, we may derive some useful information from the Hamiltonian Value Condition and the Hamiltonian Evolution Equation for this problem. From the Hamiltonian Value Condition we have, $H(t_f) = \frac{\partial \bar{E}}{\partial t_f} = \nu_t$, and from the Hamiltonian Evolution Equation we have, $\frac{d\mathcal{H}}{dt} = \frac{\partial \bar{H}}{\partial t} = 0$. Thus, for all time, $\mathcal{H}(t) = \nu_t$, a constant. The value of this constant ranges from -1 for minimum time problems to 0 for time-free problems.

The necessary conditions for problem P_S developed above may be utilized directly, as dual variables, in the generation of a candidate solution to the optimal control problem, such as in a shooting method. Alternatively, the necessary conditions may be reconstructed from the primal space. In either case the necessary conditions serve an important role in the validation of any computed solutions. In this paper, the various optimal control problems are solved using DIDO, a MATLAB toolbox for solving optimal control problems.¹⁶ DIDO implements a guess-free,¹⁷ adaptive spectral algorithm based on pseudospectral optimal control theory.¹¹ DIDO provides numerical solutions to optimal control problems wherein the dual space is reconstructed via the covector mapping theorem.¹¹ Thus, the necessary conditions derived above can be utilized in order to check the numerical results. In addition propagation tests, where optimal controls are used to drive the plant dynamics, are employed to ensure the results are feasible for implementation. Additional details on the established standard procedures for validating optimal control solutions are described in reference [16].

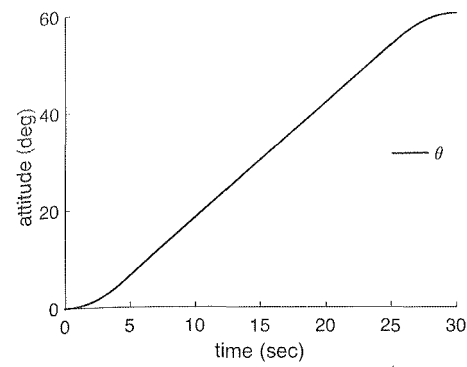
To illustrate the application of the necessary conditions to validate a solution to problem P_S , the solution for a 60-deg slew with a fixed slew time of 30-sec was obtained using DIDO. The value of $K = -0.033 \text{ kg}^{-1} \cdot \text{m}^{-2}$ was used. The results are shown in Figure 2. Referring to Figure 2, it is observed that the solution to the minimum effort problem is analogous to a standard bang-off-bang maneuver (although a momentum limit has not been explicitly given). Recall, however, that this *minimum effort* solution is based on minimizing the cumulative reaction wheel mechanical power as opposed to the true electrical power consumption of the array. However, because the profile of the minimum effort L^1 solution closely resembles that of a standard attitude maneuver (e.g. a bang-bang or bang-off-bang slew), one may erroneously conclude that current slew strategies are, in fact, power optimal. As will be demonstrated later this, however, is certainly not the case. At present, we are not interested in the solution of Figure 2 per se. On the contrary, the results of this section are presented primarily so that the main ideas behind constructing a smooth version of a L^1 optimal control formulation can be elucidated and to illustrate the utility of the necessary conditions in validating the optimality of a numerical solution to the smooth L^1 problem.

To address the latter point, consider the fact that as required by the Hamiltonian Evolution Equation, the time history of the numerical Hamiltonian (shown in Figure 2f) is a constant with value of approximately $\mathcal{H}(t) = -0.14$. This serves as one straightforward check on the optimality of the numerical solution. The trajectories for the costates and the path covectors can also be used to check against the necessary conditions and to verify that the complementarity conditions have been met. For example, the adjoint equations dictate that $\lambda_\theta(t)$ is a constant. From Figure 2d, it is seen that the value of this constant is $\lambda_\theta(t) = -3.6$. As a check on the satisfaction of the stationarity conditions, consider the fact that $\mu_\tau = -\lambda_h + \bar{h}(\mu_{\text{pos}} - \mu_{\text{neg}})$ for an optimal solution. The satisfaction of this equality by the numerical solution is illustrated in Figure 3. Satisfaction of the complementarity conditions (see equation 28) also dictates the behavior of the control variables by imposing a switching structure for the controls. Thus, optimality of the numerical solution can be further verified by confirming that the control varies in accordance with (28). This is illustrated in Figure 4 for the torque, $\bar{\tau}$. As is seen, the torque is at the lower bound when $\mu_\tau < 0$, at the upper bound when $\mu_\tau > 0$ and is zero when $\mu_\tau = 0$. Strictly speaking, the torque can take any value, $\bar{\tau} \in [\tau^L, \tau^U]$, when $\mu_\tau = 0$. However, because the torque variable appears in the cost functional, the solution admits $\bar{\tau} = 0$ for $\mu_\tau = 0$ to minimize the cost.

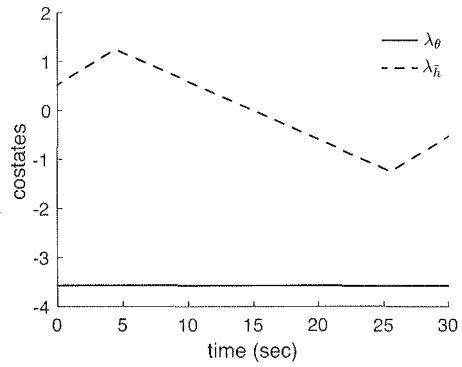
In the construction of the simplified minimum effort optimal control problem it was assumed, for convenience, that $\bar{h} = h_1 + h_2$. In order to implement the solution to slew the spacecraft, however, it is necessary to determine a momentum profile for each of the reaction wheels. One simple approach for doing this is to allocate the momentum profile given in Figure 2b to the individual wheels using a standard least-squares control allocation law, for example, the Moore-Penrose pseudoinverse. For the four-wheel array having the geometry described by (16) the pseudoinverse is given as

$$\mathbf{Z}^+ = \frac{1}{4 \cos(\eta) \sin(\eta)} \begin{bmatrix} \cos(\eta) & 0 & 2 \sin(\eta) \\ \cos(\eta) & 2 \sin(\eta) & 0 \\ \cos(\eta) & 0 & -2 \sin(\eta) \\ \cos(\eta) & -2 \sin(\eta) & 0 \end{bmatrix} \quad (36)$$

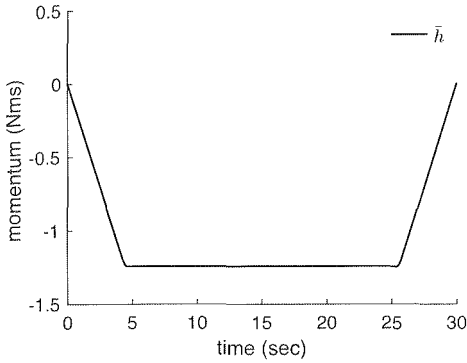
Since the solved attitude maneuver was a slew about the spacecraft body x -axis, the allocation of the required momentum profile to the wheels is straight forward. Each wheel must be commanded to produce, $h_i = \frac{1}{4 \sin(\eta)} \bar{h}$. Thus, the required momentum is allocated symmetrically to the wheels



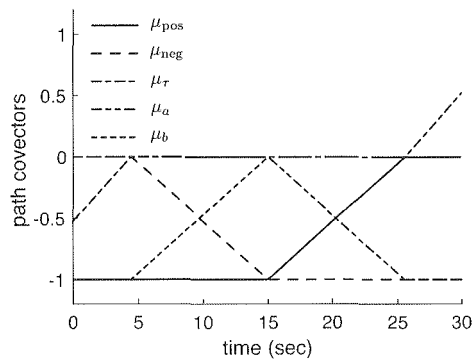
(a)



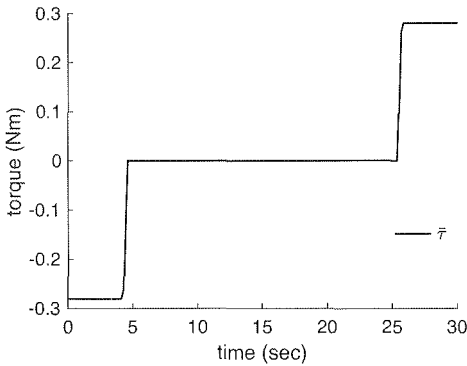
(d)



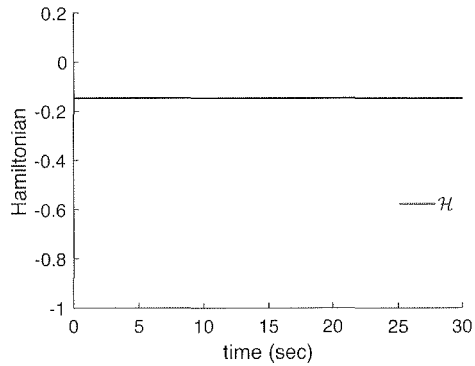
(b)



(c)



(e)



(f)

Figure 2. Solution to a L^1 minimum energy problem for a 60-deg slew about the body x -axis: (a) attitude angle; (b) momentum; (c) torque; (d) costates; (e) path covectors; (f) Hamiltonian.

so that $\frac{1}{J_w} \int_0^{t_{\text{slew}}} |\bar{\tau} \bar{h}| dt = \frac{\sin(\eta)}{J_w} \int_0^{t_{\text{slew}}} \sum_{i=1}^4 |\tau_i h_i| dt$. The time history of the running cost (integrand of the cost functional) is shown in Figure 5 along with the L^1 cost – mechanical energy input –

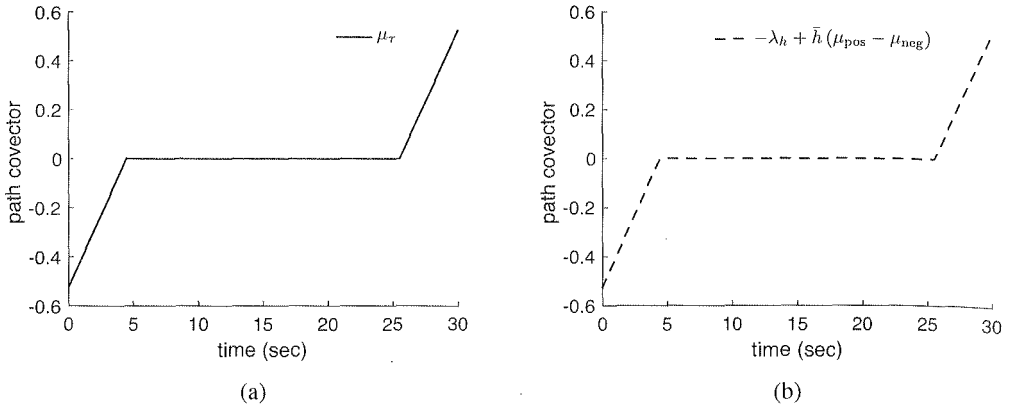


Figure 3. Verification of the stationarity condition on torque: (a) time history of path covector, μ_τ ; (b) time history of expression, $-\lambda_h + \bar{h}(\mu_{\text{pos}} - \mu_{\text{neg}})$.

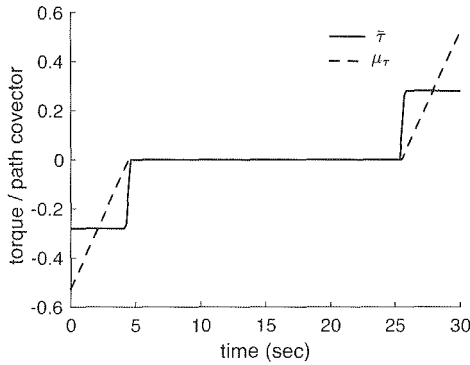


Figure 4. Verification of the complementarity condition on torque.

associated with the solution of a quadratic optimal control formulation for minimizing effort that is typically utilized in the literature. As can be seen, minimizing $\int_0^{t_{\text{slew}}} |\bar{\tau}\bar{h}|dt$ reduces mechanical energy requirements as compared to minimizing the quadratic functional, $\int_0^{t_{\text{slew}}} (\bar{\tau}\bar{h})^2 dt$. The mechanical energy input is reduced by more than 20% from 11.4 J (quadratic cost functional) to 8.9 J (L^1 cost functional). A related discussion on the difference in performance between L^1 and quadratic cost metrics can be found in [18], where it is shown that the penalty for not using the L^1 -norm is significantly more propellant consumption and undesirable continuous thrusting in a minimum-fuel spacecraft guidance and control problem.

MINIMUM POWER OPTIMAL CONTROL

In the last section, a simple *minimum effort* slew problem was developed to illustrate the procedure for transforming a nonsmooth L^1 optimal control problem into a smooth problem that could be solved by Pseudospectral optimal control theory. In the previous section the cost functional minimized the reaction wheel mechanical energy. This cost functional is, however, only a proxy for

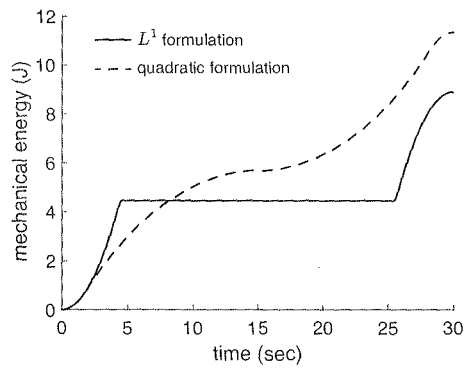


Figure 5. Mechanical energy input for a *minimum effort* attitude maneuver using L^1 and quadratic optimal control formulations.

electrical power. In this section, the *minimum power* problem is re-cast in terms of an equivalent L^1 optimal control problem so that the approach described above can be applied to formulate a problem in which reaction wheel power consumption can be minimized over a slew.

Power input to the reaction wheel array from the bus supply occurs only when the reaction wheel power equation (13) is positive. Otherwise, (13) represents the amount of heat dissipated in the ballast circuit.¹⁵ Thus, a cost functional for minimizing power should consider only the power drawn from the bus. This requirement can be met by applying the operator $\{\cdot\}^+$, described by (15), which returns only the positive part of the reaction wheel power equation for each wheel, i.e. $\mathcal{P}_i \geq 0$. Thus, a cost functional for minimizing power must properly represent the behavior of operator $\{\cdot\}^+$. An appropriate equation for calculating $\{\mathcal{P}_i\}^+$ may be written as

$$\{\mathcal{P}_i\}^+ = \frac{1}{2} (\mathcal{P}_i + |\mathcal{P}_i|) \quad (37)$$

Due to the presence of the absolute value term in (37), it is evident that a minimum power solution for a given attitude maneuver can be determined by solving an L^1 -optimal control problem involving the reaction wheel power input equation. Using this insight, a suitable minimum power optimal control problem for reaction wheel attitude control may be formulated as

$$P_{\text{PWR}} : \left\{ \begin{array}{ll} \text{Minimize} & J[\mathbf{x}(\cdot), \mathbf{u}(\cdot), t_f] = \frac{1}{2} \int_0^{t_f} (\sum_{i=1}^n \mathcal{P}_i + \sum_{i=1}^n |\mathcal{P}_i|) dt \\ \text{Subject to} & \dot{\mathbf{x}} = \left\{ \begin{array}{l} \frac{1}{2} \mathbf{Q}(\omega) \mathbf{q} \\ \mathbf{\Gamma}^{-1} \left[\begin{array}{c} -\omega \times (\mathbf{J}\omega + \mathbf{Z}\mathbf{h}) \\ \mathbf{u} \end{array} \right] \end{array} \right\} \\ & \mathbf{u} = \boldsymbol{\tau}_w \\ & \mathbf{x}(t_0) = [\mathbf{q}_0, \omega_0, \mathbf{h}_0]^T \\ & \mathbf{x}(t_f) = [\mathbf{q}_f, \omega_f, \mathbf{h}_f]^T \\ & \tau_w^L \leq \tau_{w,i} \leq \tau_w^U, \quad i = 1, 2, \dots, n \\ & h^L \leq h_i \leq h^U, \quad i = 1, 2, \dots, n \\ & \|\mathbf{q}(t)\| = 1 \\ & \|\Delta \mathbf{H}\| = 0 \\ & t_f = t_{\text{slew}} \end{array} \right. \quad (38)$$

Referring to (38), \mathcal{P}_i is the reaction wheel power input equation given by (13) for each wheel. The differential equations represent the nonlinear rotational dynamic equations of the spacecraft. Thus, point-to-point maneuvers about any rotational axis may be designed, by inserting the desired initial and final quaternions. Initial and final maneuver rates and reaction wheel momenta may also be specified via the boundary conditions. Therefore, it is possible to solve problems involving a momentum bias. This aspect is particularly important for spacecraft like the JWST because momentum accumulated by the wheels will only be periodically unloaded by thrusters. Limits on the reaction wheel torque and momentum capability are also inserted to accommodate the capabilities of the momentum control system. In the problem formulation given by (38), no bounds on spacecraft angular rate are specified. This is because the rate limit is dictated implicitly by the assumption of a fixed slew time, t_{slew} , given as part of the problem formulation. In order to design maneuvers that can be implemented on a real spacecraft system, it is also necessary to define additional constraints on the states and/or controls, such as the quaternion norm condition and the conservation of angular momentum. This is accomplished in (38), by defining additional path constraints as part of the optimal control problem formulation.

Of course, as written, problem P_{PWR} cannot be solved due to the nonsmooth cost functional. Thus, we apply appropriate transformations to convert the problem into a smooth one. For example, we may define two additional variables, $z_{a,i}$ and $z_{b,i}$ for each wheel to represent the positive and negative parts of the wheel power input. In doing so, the cost functional may be rewritten as, $J = \frac{1}{2} \int_0^{t_f} (\sum_{i=1}^n \mathcal{P}_i + \sum_{i=1}^n (z_{a,i} + z_{b,i})) dt$. The constraints, $z_{a,i} \geq 0, z_{b,i} \geq 0, z_{a,i} - \mathcal{P}_i \geq 0$, and $z_{b,i} + \mathcal{P}_i \geq 0$ must also be defined for each wheel*. The transformation into a smooth problem thus necessitates the introduction of $2n$ virtual control variables and $4n$ additional path constraints as part of the description of the smooth problem. Suffice to say, solving the smooth problem can be difficult unless the appropriate computational techniques are employed. In addition, analysis and verification of the necessary conditions becomes cumbersome. For example, the adjoint equations for the quaternions are

$$\begin{aligned}\dot{\lambda}_{q_1} &= \frac{1}{2} (\lambda_{q_2} \omega_3 - \lambda_{q_2} \omega_2 + \lambda_{q_4} \omega_1) \\ \dot{\lambda}_{q_2} &= \frac{1}{2} (-\lambda_{q_1} \omega_3 + \lambda_{q_3} \omega_1 + \lambda_{q_4} \omega_2) \\ \dot{\lambda}_{q_3} &= \frac{1}{2} (\lambda_{q_1} \omega_2 - \lambda_{q_2} \omega_1 + \lambda_{q_4} \omega_3) \\ \dot{\lambda}_{q_4} &= \frac{1}{2} (-\lambda_{q_1} \omega_1 - \lambda_{q_2} \omega_2 - \lambda_{q_3} \omega_3)\end{aligned}\tag{39}$$

Nonetheless, there are several necessary conditions for optimality that can be easily verified to validate numerical solutions including the constancy of the Hamiltonian and the complementarity conditions on the control.

APPLICATION TO THE JWST

In this section, we solve a version of the developed minimum power attitude control problem formulation to reduce the energy needed to slew the JWST. We draw our example from the work of Markley et al. [20] who present a simulated 90-deg rest-to-rest slew of the JWST using conventional

*We note that the reaction wheel power equation given by (13) contains the term, $\beta_1 \text{sign}(\Omega)$, that represents Coulomb friction. While it is possible to transform the non-differentiable $\text{sign}(\cdot)$ function into an equivalent smooth function by the introduction of additional variables and associated constraints, we instead replace the terms involving $\text{sign}(\cdot)$ with the hyperbolic tangent function, $\tanh(\cdot)$, in order to perform the smoothing operation. This assumption is justified by the fact that the error introduced by the smoothing approximation is limited to the region of zero-crossings of the reaction wheel speed. In practical applications, such zero-crossings are typically avoided, or at least minimized, to prolong the life expectancy of the wheels. Thus, the impact of the smoothing approximation on the calculation of the reaction wheel power input is considered to be negligible.

attitude control concepts. The simulation used six wheels with an elevation angle, $\eta = 35.26$ -deg, and the cone axis of the wheel configuration about the spacecraft x -axis, which is the slew axis taken in the example. Since momentum biased maneuvers are limiting, the maneuver in [20] starts with a system momentum equivalent to $2h_{\max}$ loaded in the body y -direction, where $h_{\max} = 60$ Nms is the maximum momentum that can be stored by a single wheel in the array. Representative values of the other system parameters pertinent to the momentum control system have been compiled from several open sources, e.g. references 15 and 21, and are summarized in Table 1.

Parameter	Symbol	Value	Units
Inertia tensor	\mathbf{J}	$\begin{bmatrix} 45000 & 0 & 0 \\ 0 & 90000 & 0 \\ 0 & 0 & 73000 \end{bmatrix}$	$\text{kg} \cdot \text{m}^2$
Maximum slew torque	$-\tau^L, \tau^U$	0.036	$\text{N} \cdot \text{m}$
Maximum wheel momentum	$-h^L, h^U$	60	$\text{N} \cdot \text{m} \cdot \text{s}$
Wheel inertia	J_w	0.13	$\text{kg} \cdot \text{m}^2$
Wheel Coulomb friction	β_1	0.002	$\text{N} \cdot \text{m}$
Wheel viscous friction	β_2	5×10^{-5}	$\text{N} \cdot \text{m} / \text{rad} / \text{s}$
Motor torque constant	K_T	0.07	$\text{N} \cdot \text{m} / \text{A}$
Motor back-EMF constant	K_Ω	0.07	$\text{V} / \text{rad} / \text{s}$
Motor bridge resistance	R_M	1.8	Ohms
Bus voltage	V_s	28	V
Harness resistance	R_h	0.004	Ohms
Quiescent power	P_q	3.0	W

Table 1. Representative parameters of the JWST momentum control system.^{15, 19, 20, 21, 22}

In order to reconstruct the baseline slew simulation, equation (17) may be rewritten to accommodate the momentum bias term

$$\mathbf{J}\boldsymbol{\omega} + \mathbf{Z}\mathbf{h} = \begin{bmatrix} 0 \\ 2h_{\max} \cos(\theta) \\ -2h_{\max} \sin(\theta) \end{bmatrix} \quad (40)$$

Equation (40) can be expanded similarly to (19) to give

$$\begin{bmatrix} \omega_x \\ \frac{4 \cos(\theta)}{\sqrt{3} \cos(\eta)} h_{\max} \\ -\frac{\sin(\theta)}{\cos(\eta)} h_{\max} \end{bmatrix} = \begin{bmatrix} -\frac{1}{J_{xx}} \sin(\eta) (h_1 + h_2 + h_3 + h_4 + h_5 + h_6) \\ h_2 + h_3 - h_5 - h_6 \\ 2h_1 + h_2 - h_3 - 2h_4 - h_5 + h_6 \end{bmatrix} \quad (41)$$

Since it is customary to design slew maneuvers without regard to momentum bias, the value of h_{\max} may be set to zero in (41). After doing so, and after some algebraic manipulation, a simplified model of conventional attitude maneuver can be written in precisely the same form as (20)

$$\begin{bmatrix} \dot{\theta} \\ \dot{h} \end{bmatrix} = \begin{bmatrix} -\frac{1}{J_{xx}} \sin(\eta) \bar{h} \\ \bar{\tau} \end{bmatrix} \quad (42)$$

but, in this case, with $\bar{h} = h_1 + 2h_2 + 2h_3 + h_4$ and $\bar{\tau} = \tau_1 + 2\tau_2 + 2\tau_3 + \tau_4$. The conventional attitude maneuver can now be determined by solving the *minimum effort* problem described earlier using the new definitions for \bar{h} and $\bar{\tau}$. Doing so yields a reaction wheel momentum profile that does

not consider the momentum bias. However, the reaction wheel momentum profile with bias may be reconstructed by rearranging (40) and solving the resulting equation as a function of time

$$\mathbf{h} = \mathbf{Z}^+ \left(-\mathbf{J}\boldsymbol{\omega} + \begin{bmatrix} 0, & 2h_{\max} \cos(\theta), & -2h_{\max} \sin(\theta) \end{bmatrix}^T \right) \quad (43)$$

In (43), the conventional Moore-Penrose allocation is assumed for matrix \mathbf{Z}^+ .

The resulting solution to the *minimum effort* problem is shown in Figure 6. In solving the minimum effort problem, the slew time was taken as $t_{\text{slew}} = 36$ -minutes (as in reference [20]) because several wheels, i.e. wheels 1 and 6, are observed to reach the momentum limit. Thus, the slew cannot be completed more quickly without saturating the wheels. The maneuver profiles are shown in Figure 6 is precisely the same as the conventional slew profile presented previously in [20], though in the previous work the slew was designed by applying the standard template associated with a conventional Eigenaxis slew maneuver. In other words, the maneuver in [20] was designed from the point of view of kinematics, by assuming a bang-off-bang angular acceleration profile and not by solving an L^1 optimal control problem.

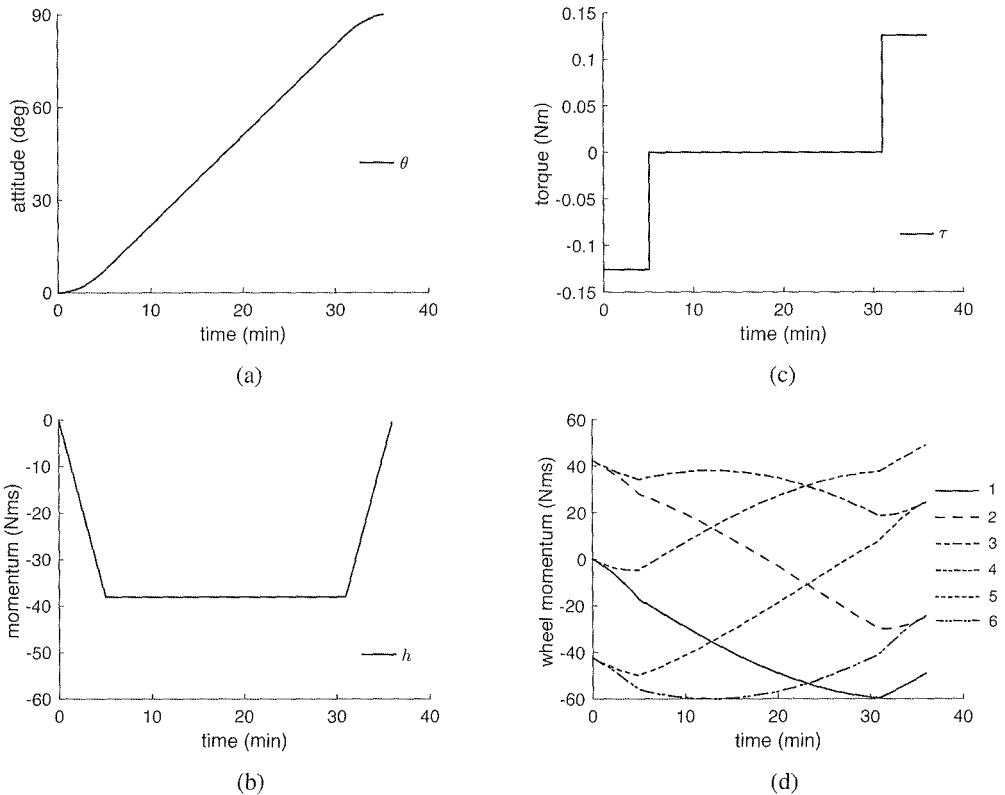


Figure 6. Conventional maneuver profiles for a 90-deg rest-to-rest slew of the JWST: (a) attitude angle; (b) slew momentum; (c) slew torque; (d) Moore-Penrose momentum distribution.

The *minimum power* problem for reaction wheel maneuvering was solved next for the same 90-deg x -axis slew as in the baseline maneuver described above. The same time horizon was assumed.

As part of the problem formulation, momentum constraints were also included to enforce an Eigenaxis motion. In other words, it was assumed that off-Eigenaxis motions, while potentially advantageous, were not allowed. The resulting maneuver profiles are shown in Figure 7. The Hamiltonian associated with the numerical solution is shown in Figure 8. As is seen the Hamiltonian is nominally constant as a function of time, indicating that an extremal solution satisfying the necessary conditions for optimality has been determined. Referring to Figure 7 it is seen that the *minimum power* solution differs from the baseline solution in two ways: (i) The time-history of the momentum profile about the spacecraft body x -axis has changed due to the application of a different body x -axis torque – the minimum power maneuver is no longer bang-off-bang, and (ii) the momentum profiles of the individual wheels have changed significantly from those seen in the baseline solution (compare Figure 6d with Figure 7d). The difference between Figure 6d with Figure 7d) represents the re-distribution of momentum necessary to reduce the overall reaction wheel input power needed to complete the maneuver.

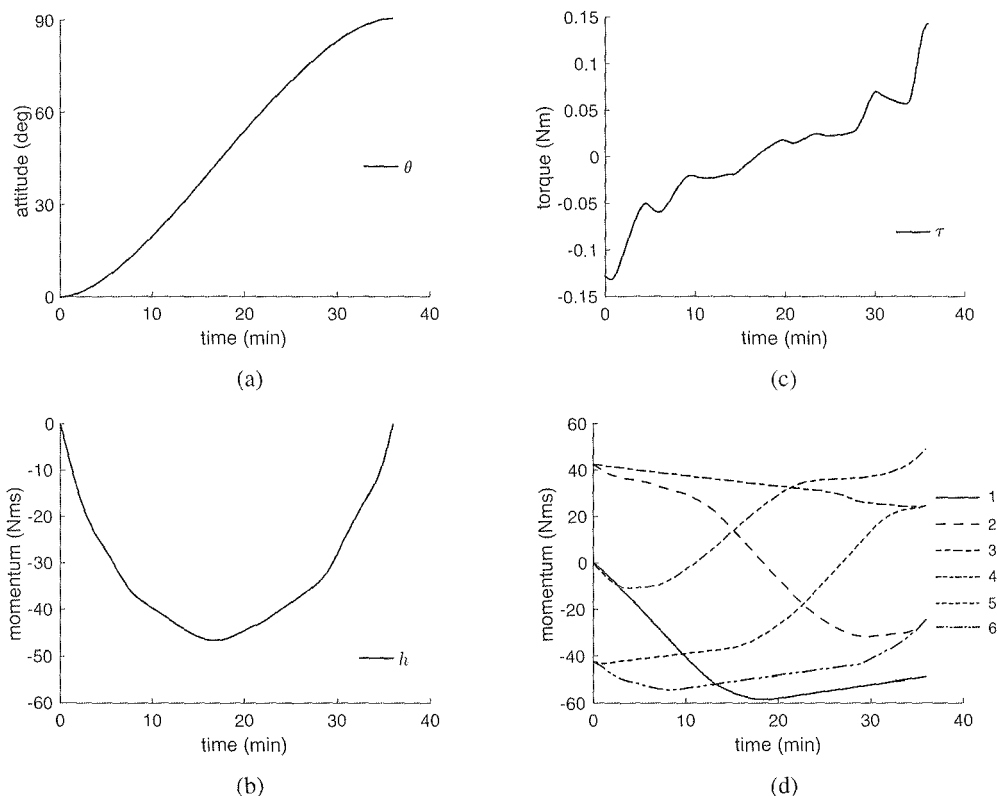


Figure 7. Minimum power maneuver profiles for a 90-deg rest-to-rest slew of the JWST: (a) attitude angle; (b) slew momentum; (c) slew torque; (d) minimum power momentum distribution.

To illustrate the reduction in reaction wheel power that can be achieved by solving the minimum power optimal control problem, the time-histories of the total instantaneous power input to the reaction wheel array for the baseline and minimum power solutions are plotted in Figure 9. The cumulative power consumption (integrated power) over the slew is also shown so that the total

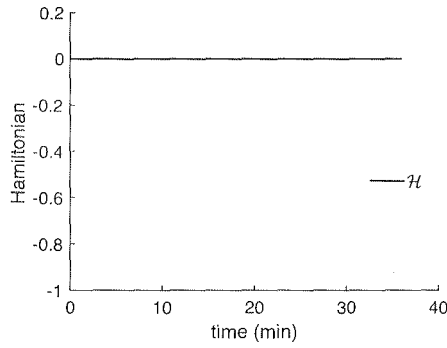


Figure 8. Hamiltonian associated with the minimum power maneuver of Figure 7.

energy can be determined. As can be seen, the minimum power momentum distribution considerably reduces reaction wheel power input for the slew maneuver. In particular, the peak power of the array is reduced by 22% from 52 W for the conventional maneuver to 40 W for the new minimum power solution (see Figure 9a). It is also evident that for the minimum power solution, the peak-to-average power draw ratio has been improved. Referring to Figure, 9b, the total energy consumption is reduced by 20% from 62 kJ for the conventional maneuver to 50 kJ for the new minimum power solution. While it was not done here, the peak power of individual wheels may be limited by introducing an appropriate upper bound on variables, z_a and z_b , in problem P_{PWR} . Similarly, energy consumption of individual wheels may be limited by introducing isoparametric constraints (see reference [16, 23]) as part of the optimal control problem formulation.

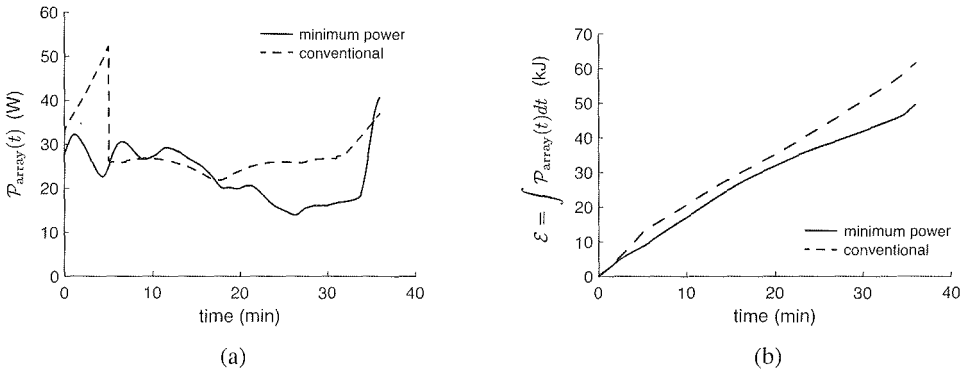


Figure 9. Reduction in reaction wheel power input for conventional Moore-Penrose momentum distribution and new minimum power momentum distribution: (a) instantaneous array power; (b) cumulative array energy.

CONCLUSIONS

This paper described a minimum power optimal control formulation for reducing the slew energy requirements of a reaction wheel spacecraft. While previous work focuses on minimizing proxies for reaction wheel power, the formulation developed here operates directly on the power input

equation. In order to avoid issues associated with non-differentiable functions, the introduction of appropriate functional constraints and transformations was used to build a smooth cost functional for reaction wheel power. The resulting L^1 optimal control problem could then be solved using Pseudospectral optimal control theory. Application for a typical large-angle slew of the James Webb Space Telescope showed that the minimum power solutions can significantly reduce requirements as compared to conventional attitude control concepts. The energy reduction ($\sim 20\%$) was obtained by finding a minimum power momentum distribution that achieves the necessary control effort to slew about the Eigenaxis, while simultaneously reducing the overall power input to the individual wheels. Reducing the power demands of reaction wheels during spacecraft attitude slews can have multiple benefits both in the up-front spacecraft design phase as well as during in-flight operations, ranging from mass savings on the batteries and power distribution system to lowering the thermal stresses within the wheels, which may prolong the mission life.

REFERENCES

- [1] Schaub, H. and Lappas, V. J., "Redundant Reaction Wheel Torque Distribution Yielding Instantaneous L^2 Power-Optimal Spacecraft Attitude Control," *Journal of Guidance, Control, and Dynamics*, Vol. 32, No. 4, 2009, pp. 1269–1276.
- [2] Blenden, R. and Schaub, H., "Regenerative Power-Optimal Reaction Wheel Attitude Control," *Journal of Guidance, Control, and Dynamics*, Vol. 35, No. 4, 2012, pp. 1208–1217.
- [3] Skaar, S. and Kraige, L., "Single-Axis Spacecraft Attitude Maneuvers Using an Optimal Reaction Wheel Power Criterion," *Journal of Guidance, Control, and Dynamics*, Vol. 5, No. 5, 1982, pp. 543–544.
- [4] Skaar, S. and Kraige, L., "Large-Angle Spacecraft Attitude Maneuvers Using an Optimal Reaction Wheel Power Criterion," *Journal of the Astronautical Sciences*, Vol. 32, No. 1, 1984, pp. 47–61.
- [5] Wehrend, W. R., "Minimum Energy Reaction Wheel Control for a Satellite Scanning a Small Celestial Area," NASA TN D-392, 1967.
- [6] Dueri, D., Leve, F., and Acikmese, B., "Minimum Error Dissipative Power Reduction Control Allocation via Lexicographic Convex Optimization for Momentum Control System," *IEEE Transactions on Control Systems Technology*, Vol. 24, No. 2, 2016, pp. 678–686.
- [7] Marsh, H., Karpenko, M., and Gong, Q., "Energy Constrained Shortest-Time Maneuvers for Reaction Wheel Satellites," AIAA/AAS Astrodynamics Specialist Conference, September 13 – September 16, 2016, Long Beach, CA. AIAA paper: AIAA 2016-5579.
- [8] Dennehy, N., "Spacecraft Hybrid Control at NASA: A Look Back, Current Initiatives, and Some Future Considerations," *Proceedings of the 37th Annual AAS Guidance and Control Conference*, January 31 – February 5, 2014, Breckenridge, CO. AAS paper: AAS-14-101.
- [9] Clarke, F. H., Ledyev, Y. S., Stern, R. J., and Wolenski, P. R., *Nonsmooth Analysis and Control Theory*, Springer-Verlag, New York, 1998.
- [10] Clarke, F. H., *Optimization and Nonsmooth Analysis*, SIAM, Philadelphia, PA, 1990.
- [11] Ross, I. M. and Karpenko, M., "A Review of Pseudospectral Optimal Control: from Theory to Flight," *Annual Reviews in Control*, Vol. 36, No. 2, 2012, pp. 182–197.
- [12] Sabelhaus, P. A., Campbell, D., Clampin, M., Decker, J., Greenhouse, M., Johns, A., Menzel, M., Smith, R., and Sullivan, P., "An Overview of the James Webb Space Telescope (JWST) Project," *Proceedings of the SPIE 5899, UV/Optical/IR Space Telescopes: Innovative Technologies and Concepts II*, 2005. Paper number: 58990P.
- [13] Stoneking, E., "Newton-Euler Dynamic Equations of Motion for a Multi-Body Spacecraft," AIAA Guidance, Navigation and Control Conference, August 20–23, 2007, Hilton Head, SC. AIAA paper: AIAA-2007-6441.
- [14] Sidi, M. J., *Spacecraft Dynamics and Control*, Cambridge University Press, New York, 1997.
- [15] Bialke, B., "High Fidelity Mathematical Modeling of Reaction Wheel Performance," AAS Guidance and Control Conference, February 4 – February 8, 1998, Breckenridge, CO. AAS paper: AAS-98-063.
- [16] Ross, I. M., *A Primer on Pontryagin's Principle in Optimal Control*, Second Edition, Collegiate Publishers, San Francisco, CA 2015.
- [17] Ross, I. M. and Gong, Q., "Guess-Free Trajectory Optimization," AIAA/AAS Astrodynamics Specialist Conference and Exhibit, August 18–21, 2008, Honolulu, HI. AIAA paper: 2008-6273.

- [18] Ross, I.M., "How to Find Minimum-Fuel Controllers," *AIAA Guidance, Navigation, and Control Conference and Exhibit*, Providence, RI, 2004, AIAA paper: AIAA 2004-5346.
- [19] Ahronovich, E., and Balling, M., "Reaction Wheel and Drive Electronics for LeoStar Class Vehicles," Small Satellite Conference, Logan, UT, 1998. Paper number: SSC98-I-5.
- [20] Markley, F. L., Reynolds, R. G. , Liu, F. X., and Lebsock, K. L., "Maximum Torque and Momentum Envelopes for Reaction Wheel Arrays," *Journal of Guidance, Control, and Dynamics*, Vol. 33, Oct. 2010, pp. 1606–1614.
- [21] Meza, L., Tung, F., Anandakrishnan, S., Spector, V., Hyde, T., "Line of Sight Stabilization of James Webb Space Telescope," *Proceedings of the 27th Annual AAS Guidance and Control Conference*, Breckenridge, CO, 2005. AAS paper: AAS-05-002.
- [22] Kinzel, W. M. and Isaacs, J., "Momentum Management Operations Concept," JWST Observatory Technical Report - JWST-STScI-001275. Available online: <http://www.stsci.edu/jwst/doc-archive/technical-reports>. Retrieved: 26 January, 2015.
- [23] Bryson, A. E. and Ho, Y. C., *Applied Optimal Control*, Hemisphere, New York, 1975.